Proceedings of the ASME Turbo Expo 2020
Turbomachinery Technical Conference and Exposition
GT2020
June 22-26, 2020, ExCeL London Convention Center, London, United Kingdom

GT2020-15683

COMPUTATIONAL INVESTIGATION OF A MULTIPHASE TURBO EXPANDER FOR HEAT PUMPS AND REFRIGERATION CYCLES

Zoitis Giakoumis[1], E. Geoffrey Engelbrecht[1], Alexandros Chasoglou[2], Ndaona Chokani[2]

[1]Limmat Scientific AG, Industriestrasse 7, CH-6300, Zug, Switzerland
[2]Laboratory for Energy Conversion, ETH Zürich, Department of Mechanical and Process Engineering, Sonneggstrasse 3, CH-8092, Zurich, Switzerland

ABSTRACT

The design and development of an innovative Tesla style turbo expander for two-phase fluids is proposed, as a substitute for the lamination valve of a traditional Heat Pump cycle. Thereby enhancing the overall performance of the Heat Pump, by recovering mechanical work to offset the compressor requirements. The major challenge in such configurations is the reliable operation of the expander, when phase change occurs across it, from a purely liquid flow to a mainly vapour flow by volume with a dense cloud of liquid droplets.

To investigate the phase change, a modelling approach is adopted which is routinely applied to modelling fuel-flashing in direct injection diesel engines, where the phase change deviates strongly from equilibrium. The Homogeneous Relaxation Model (HRM) is employed, which utilizes an Eulerian approach.

The proposed computational model is firstly validated against experimental results available in the literature. A sensitivity analysis of the phase change model relaxation parameter is performed. It was found that a value 10 times lower than the published value gave closer agreement to the measured results. It is believed that this result is due to the roughened walls of the experiment, which would produce more nucleation sites for vapour bubble formation. This suggests that this model maybe is sensitive to the geometry of the turbine.

Following this validation, the detailed flow profile in the proposed Tesla turbo-expander is investigated. Two different expander designs are considered in this project, one working with water [4,20] and the other with butane (R600). This study focuses particularly on the butane expander design. The expander performance is evaluated for rotational speeds up to 32'000 RPM.

Results on the turbo-expander under investigation, showed that the presence of a dense cloud of liquid droplets produces a significant pressure drop across the turbine rotor, which increases with RPM, postponing the phase change. High volume-fraction of liquid was predicted to penetrate deeper inside the rotor above 16'000 RPM for the butane expander. The resulting lower liquid flow velocity relative to the rotor disk speed at the inlet of the rotor is predicted to significantly degrade the performance of the turbine at high rotational speeds. Decreasing the nozzle throat area improves the situation, by initiating the phase change further upstream and increasing the RPM operational range by 50%. Angling the nozzle radially inward by 10° was found to not have a great impact on the performance of the turbine. It was determined from this study that it is critical to predict correctly where the phase change starts, in order to accurately predict the performance of the turbine. Important is to remove as much liquid as possible from the flow, before it enters the rotor, to minimize the impact of the phase change on the turbine performance.

Keywords: Tesla Turbine, Multiphase Flow, Heat Pump, Refrigeration Cycle, Numerical Modelling, CFD

NOMENCLATURE

x	Vapour mass fraction generation
$\bar{x}$	Equilibrium vapour mass fraction
ρ	Density of the mixture
Θ	Local relaxation time scale
t	Time
h	Specific mixture enthalpy
$h_{sat,l}$	Liquid specific enthalpy at saturated condition
$h_{sat,v}$	Vapour specific enthalpy at saturated condition
Θ_0	relaxation time scale constant
ε	Vapour volume or void fraction
ψ	Non-dimensional pressure difference
ρ_l	Density of the liquid phase
ρ_v	Density of the vapour phase
P	Local static pressure
P_s	Local saturation pressure
Deg. , °	Degrees
BC	Boundary condition
RPM	Rotational speed (revolutions per minute)

HRM	Homogeneous relaxation model
HRM/ct.	Homogeneous relaxation model with different relaxation time scale constant, θ_0/ct

1. INTRODUCTION

Throughout the world most commercial applications of heat pumps or refrigeration cycles use a Joule Thomson expansion valve between the condenser and evaporator. This can result in wasted energy of 10-20% of the system power. Thereby energy produced by the flow expansion, could be potentially conserved by a turboexpander (Figure1).

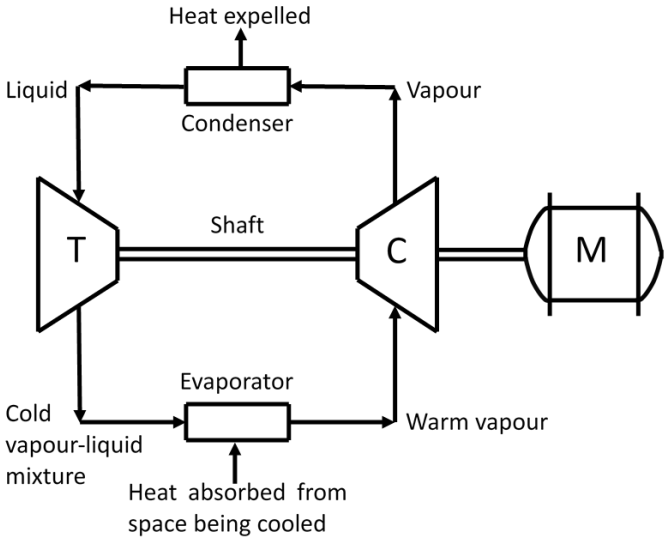

Figure 1. Turboexpander in Refrigeration Cycle

One reason that turboexpanders are not commonly used in these cycles, is that usually during the flow expansion a partial phase change occurs. The flow typically enters the nozzle as a liquid or sometimes as a two-phase or supercritical fluid. Then it exits primarily as vapour, by volume, with a dense cloud of liquid droplets. Through the flow expansion liquid droplets face an adverse centrifugal force field, that incurs the risk of erosion and vibration to the turbine blades. The expansion also often leads to separation of the liquid phase from the driving vapour phase, causing slip and frictional losses. Spezia *et al* [1] proposed the implementation of a turboexpander in place of the expansion valve, based on the Tesla turbine [2] (Figure 2). Steidel *et al* [3] also evaluate the performance of a Tesla turbine for geothermal applications with phase change, in which the flow expansion happens in a similar way.

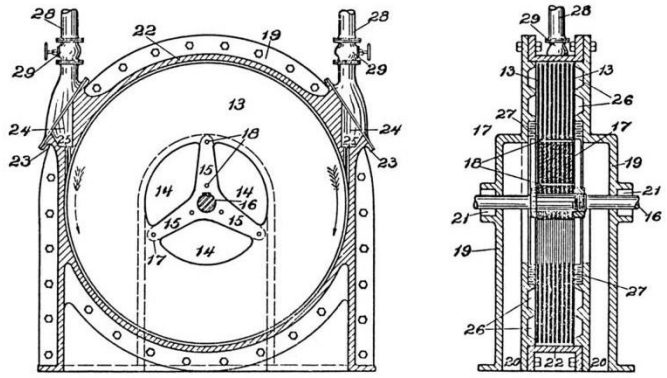

Figure 2. Tesla Turbine (by Tesla U.S Patent 1913)

This type of turbine consists of a set of closely spaced disks. Nozzles at the outer edge of the disks produce a tangentially moving fluid, that enters the space between the disks and spirals towards the center, exiting from an exhaust near the axis of the disks. Because of the tangential orientation of the nozzles, a vortical flow is generated between the disks. The fluid drags on the disks, by means of viscosity and adhesion of the surface layer of the fluid. In this way, the disks pick up energy from the flow through the boundary layer and start spinning. Because this turbine extracts energy from the boundary layer, the only surface that is potentially exposed to collision and hence erosion from liquid droplets, is the one located at the outer edge of the disks. Due to the fact that the local speed of sound strongly depends on the vapour mass fraction and also because the phase change has an impact on the temperature and density, it is critical to accurately predict the rate of phase change within the expander, in order to obtain a reasonable prediction of the turbine performance.

To validate the modelling approach adopted to predict the non-equilibrium phase change, first simulations were performed against a simple nozzle with water as a working fluid from the work of Park *et al* [18]. Next simulations were performed by Engelbrecht *et al* [4], of a static Tesla turbine test rig comprised of a single passage between two disks using water as a working fluid. This test rig is being developed by Traverso *et al* [20], but has not yet been commissioned. Thus as testing has not yet been performed, a broad parametric study of the influence of model parameters on the performance of the turbine was carried out, which will be summarized later. A second dynamic test rig consisting of 120 disks, which uses butane (R600) as a working fluid is being constructed as a prototype to test the feasibility of this concept. The study reported here, presents the initial modelling carried out to assist the development of this turbine. To this end the main aim of this study is to assess the qualitative impact of the phase change on the performance of the turbine.

2. BUTANE TESLA EXPANDER

The butane expander design analyzed in this study, is based on a test rig, which will be constructed at the University of Genoa within the framework of the European Union Horizon 2020 funded project, PUMP-HEAT. As the ultimate aim of the study is to design an operational Tesla turbine, the initial modelling assesses a range of rotational speeds, nozzle angles and nozzle throat areas. The expander design geometry for the large nozzle throat area is depicted in Figure 3.

The expander consists of two nozzles at the outer edge of the disks, that are spaced 180 Deg. apart. Through these nozzles liquid butane is provided to the Tesla expander at 0.5 MPa and

26.8°C. The majority of the resulting liquid vapour mixture exits the expander at 0.07 MPa, through a central shaft at the inner radius of the disk. The expander is composed of a set of 120 disks, with an individual disk thickness equal to 0.075 mm and a gap between the disks similarly equal to 0.075 mm. The circular disks have an inner diameter of 24 mm and outer diameter of 40 mm. The minimum clearance between the disks and casing is 0.1mm and the throat area of the nozzle is equal to 31.2 mm^2.

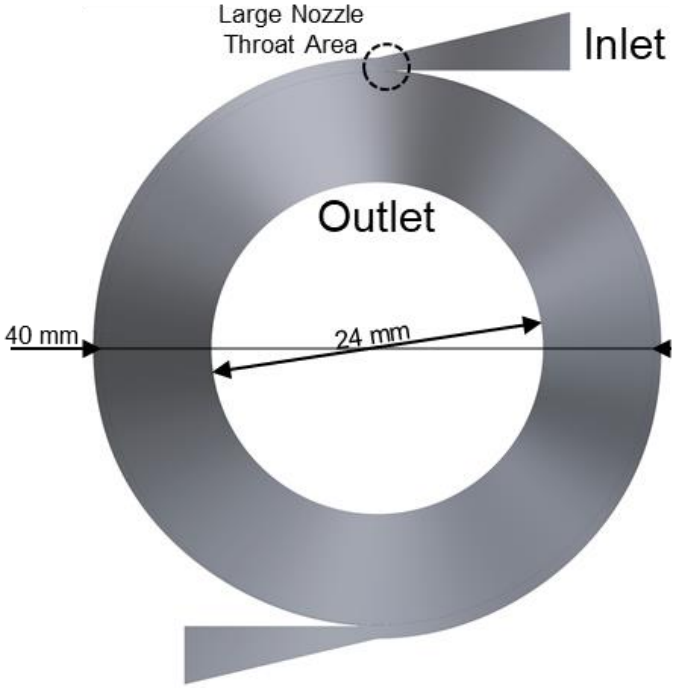

Figure 3. Expander with Large Nozzle Throat Area

Furthermore for investigating the influence of the nozzle throat area on the performance of the turbine, a smaller throat area was used which is depicted in Figure 4.

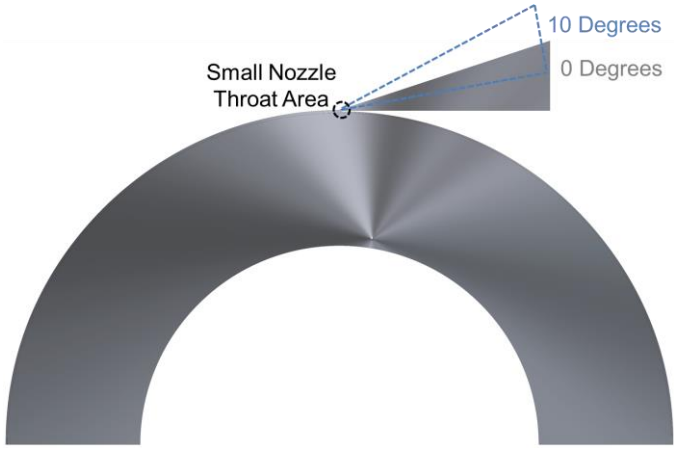

Figure 4. Expander with Small Nozzle Throat Area: 0 Deg. & 10 Deg. Nozzle Angle

As it appears in the 180° section, the expander design geometry has the same geometrical characteristics in the rotor, as in the large nozzle throat area geometry. The only difference exists in the nozzle, where the nozzle throat area is decreased by modifying the casing outer wall radius. Moreover in order to assess the impact of the nozzle angle on the performance of the Tesla turbo expander, a second nozzle was considered, only for the small throat area case with a 10 Deg. angle. The change of the nozzle angle although comes along with a slight adjustment in the nozzle throat area, in order to maintain the same mass flow in both 0 and 10 Deg. nozzle angle cases. The 0 Deg. and 10 Deg. nozzle finally led to a throat area of 1.8 mm^2 and 1.48 mm^2 respectively. In that way, the impact of varying the nozzle throat area (large & small) and angle (0 & 10 Deg.) on the phase change process could be investigated in detail. Finally with the purpose of reducing the computational time and cost, a periodic 180° section of half of one disk passage with a single nozzle was finally modelled and not the full turbo expander (Figure 5).

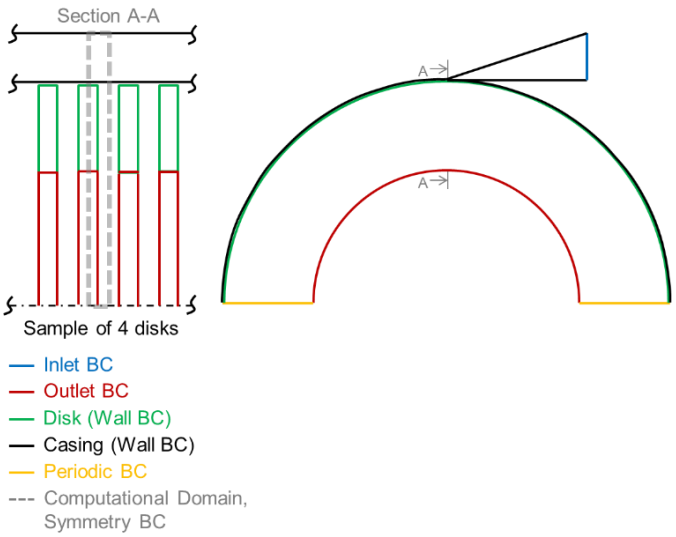

Figure 5. Computational Domain of the Expander

The computational domain consists of a half disk with half the space between 2 consecutive disks, as it is depicted in Section A-A of Figure 5. Furthermore the boundary conditions, which remain constant in the whole study, are highlighted in this figure. Specifically, the inlet total pressure and temperature were set as 0.5 MPa and 26.8°C and the outlet static pressure was set as 0.07 MPa. All the walls were treated as smooth walls. Symmetry boundary conditions were chosen at the sides of the domain, to model a disk passage in the middle of the turbine, where axial flow would be negligible. Thus losses incurred, due to the sides of the turbine, were not considered in this analysis.

A hybrid unstructured grid of 12 million nodes, with y+ values of less than 1 over most of the domain and less than 4 over all of the domain, was used for the analysis (Figure 6).

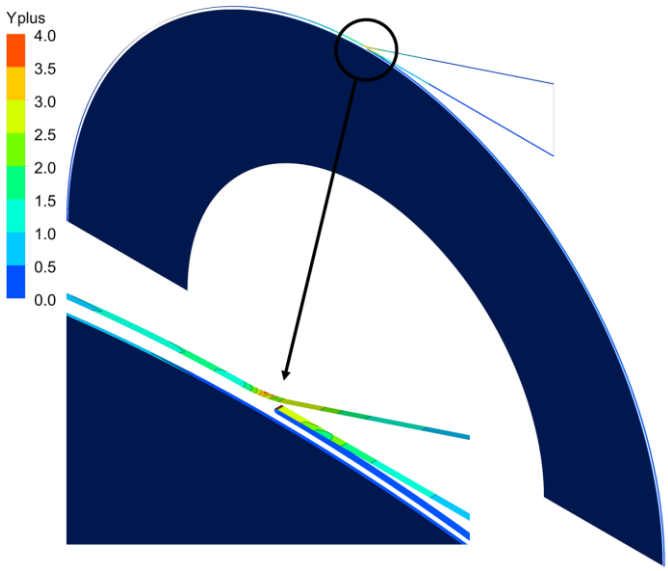

Figure 6. Yplus Values of the Computational Domain

Given the uncertainty of the phase change model, which will be discussed later and will likely be the biggest source of error in the analysis, a grid sensitivity study was not performed for this specific case, as the study intends to be qualitative in nature with major interest in the relative trends and impact of the phase change on the performance of the turbine. However, extensive experience from previous turbomachinery simulations was applied and the mesh resolution was adapted to resolve the boundary layer and areas of the flow, where steep gradients were expected.

Predicated on the inlet and outlet condition, the idealized operating line of the turbine for an isentropic expansion can be seen in Figure 7.

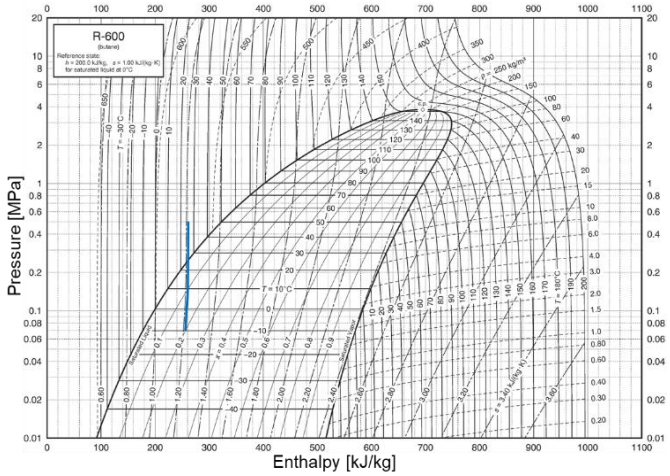

Figure 7. Operating Line of the Turbine without Losses (by Miyamoto and Watanabe 2001)

As it is shown in the pressure-enthalpy chart [23], it's expected that the steam exiting the turbine will have a quality of approximately 20%.

3. MODEL

CFX is used to solve the Reynolds averaged Navier-Stokes equations. The SST (Shear Stress Transport) model [5] is used to close the Reynolds Stresses. All working fluids are modelled as real fluids, with properties for water taken from the IAPWS IF97 steam tables and properties of butane taken from the NIST database.

To accurately model inhomogeneity effects between the momentum of the liquid and vapour phases, droplet sizes are required to be known. Given the computational limits, a reliable simple way to model this could not be found and because of the absence of experimental data, we have opted to make the assumption of homogeneity. To assess the impact of this assumption, Engelbrecht *et al* [4] investigated inhomogeneity effects for a range of possible droplet sizes, in the context of a Tesla turbine operating with water as a working fluid. Essentially they found that as droplet size increases, the liquid phase would be more strongly influenced by the centrifugal forces within the rotor, compared to the vapour phase, taking a longer flow path to the exit. This resulted in an increase in the liquid phase concentration within the rotor, increasing the resistance of the flow through the rotor and hence increasing the pressure drop across the rotor. The homogeneous case, which is equivalent to infinitely small droplets, had the lowest pressure drop across the rotor. This should be considered when interpreting the results of this study.

To model the non-equilibrium phase change, an approach is adopted, which has been applied successfully over the last decade to model fuel flash atomization in gasoline direct injection engines [6-14]. The HRM (Homogeneous Relaxation Model) was first proposed by Bilicki *et al* [15] and later extended by Downar-Zapolski *et al* [16], to model the influence of non-equilibrium effects on the vapour formation rate during the flash boiling of water. The model proposes that the deviation from equilibrium can be solved with an assumed linear approximation, or equally the first term in a Taylor series expansion, of the vapour mass fraction generation x:

$$\frac{Dx}{Dt} = -\rho \frac{x-\bar{x}}{\Theta} \tag{1}$$

where $\bar{x}$ is the equilibrium vapour mass fraction, ρ is the density of the mixture and Θ is the local relaxation time scale over which x tends to $\bar{x}$. The equilibrium vapour mass fraction can be expressed as

$$\bar{x} = \frac{h-h_{sat,l}(P)}{h_{sat,v}(P)-h_{sat,l}(P)} \tag{2}$$

where h corresponds to the mixture specific enthalpy, while $h_{sat,l}(P)$ and $h_{sat,v}(P)$ are for the liquid and vapour specific enthalpies at saturated conditions.

The relaxation time Θ is modelled by an empirically derived correlation proposed by Downar-Zapolski *et al* [16], based on Reocreux's measurements of water flashing in a pipe for pressure drops below 10 bar [17]. The correlation for the relaxation time has the form

$$\Theta = \Theta_0 \varepsilon^{-0.257} \psi^{-2.24} \quad (3)$$

where $\Theta_0 = 6.51 \times 10^{-4}$ has the dimension of time in seconds and ε is the vapour volume or void fraction given by:

$$\varepsilon = \frac{x\rho_l}{\rho_v + x(\rho_l - \rho_v)} \quad (4)$$

where ρ_l and ρ_v are the densities for the liquid and vapour phase respectively. Also ψ is the non-dimensional pressure difference expressed by:

$$\psi = \frac{P_s(T) - P}{P_s(T)} \quad (5)$$

where $P_s(T)$ and P are the local saturation pressure and local static pressure respectively.

3.1 Model Validation

To validate the modelling approach, predictions were compared against measurements made by Park *et al* [18] at similar operating conditions for a simple rectangular nozzle with water as the working fluid, which exhausted into a large chamber at atmospheric pressure (Figure 8).

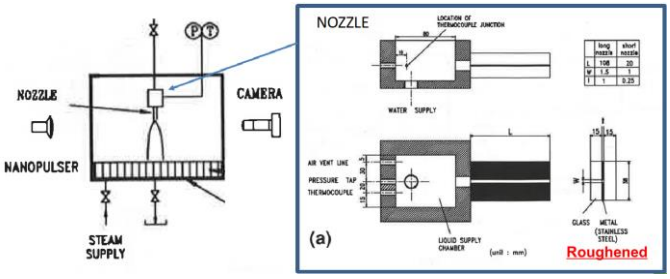

Figure 8. Steam Rectangular Nozzle (by Park and Lee 1994)

As is depicted in Figure 9, the published HRM underpredicted the spray angle for a range of inlet temperatures at an inlet pressure of 0.4 MPa. The spray angle was found to increase as the phase change moved closer to the nozzle outlet. Thus this indicates that the original HRM is predicting the phase change to be too far downstream. Reducing Θ_0 by an order of magnitude (HRM/10) gave a better agreement for the spray angle for inlet pressures of both 0.3 and 0.4 MPa. Additionally the inflection point at 120 °C, which appears to occur when significant phase change reaches the nozzle outlet, was captured with this value of Θ_0.

This mismatch may be in part, due to the fact that the stainless steel walls of Park *et al's* nozzle were roughened with 800 mesh sandpaper. This will potentially increase the number of nucleation sites for vapour bubble formation, accelerating the rate of phase change.

Given the uncertainty of this model constant and in the absence of better validation from the static Tesla test rig, which has yet to be run, sensitivity analysis of this parameter is performed for all of the analysis.

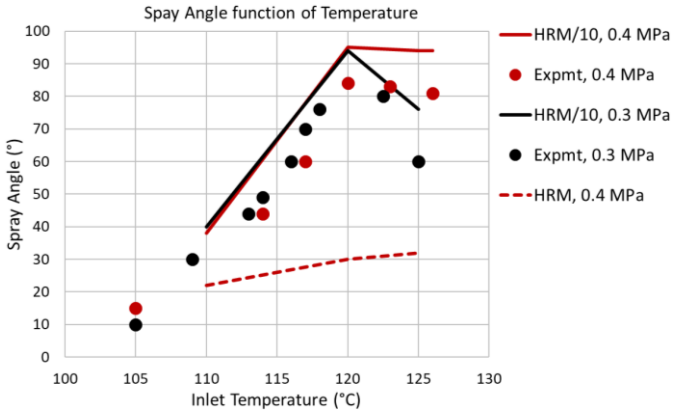

Figure 9. Spray Angle Evaluation with HRM

This model has only been validated in this study against water as a working fluid, as it was reported earlier. Although it is widely used in the literature for gasoline flashing, thus it was deemed appropriate to be applied to the butane analysis.

3.2 Analysis

The simulations were performed on a 180° periodic sector of the proposed butane Tesla expander, firstly for the large nozzle throat area case and then for the small nozzle throat area case of 0 Deg. and 10 Deg. nozzle angle respectively. All of the simulations were performed with an inlet pressure of 5 bar and temperature of 300 K and an outlet pressure of 0.7 bar. Taking into consideration the uncertainly of the model, the published HRM as well as HRM/10 were considered for all of the design cases.

4. RESULTS

Considering first the influence of the design parameters on the predicted rotor torque, Figure 10 is shown. Reducing the nozzle throat area for a constant pressure drop, has the effect of reducing the mass flow through the turbine. Thus it is understandable that the torque is much higher for the case with the largest nozzle throat area. However it is interesting to note that the torque is predicted to reach zero at a much lower RPM, than for the cases with a smaller nozzle throat area. The impact

of angling the nozzle is not large, since the RPM where the torque reaches zero doesn't differ that much. The HRM/10 cases are all predicted to have slightly lower torque at low RPM, but then to have a smaller slope reaching zero RPM at a significantly higher RPM.

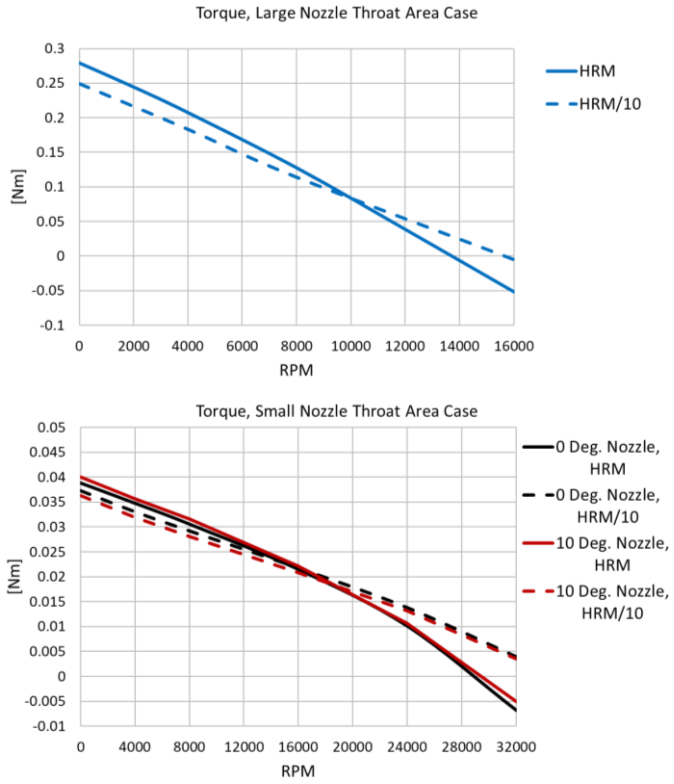

Figure 10. Torque vs RPM

The HRM/10 torque is slightly lower compared to the original HRM at low RPM, due to the lower mass flow through the nozzle (Figure 11). As the phase change is closer to the nozzle outlet for the HRM/10 case, the volume expansion of the vapour formation produces a bigger blockage for the flow, reducing the mass flow. As a consequence of the predicted torque behavior, the optimal RPM for maximum power varies as a function of the nozzle throat area and rate of the phase change (Figure 12).

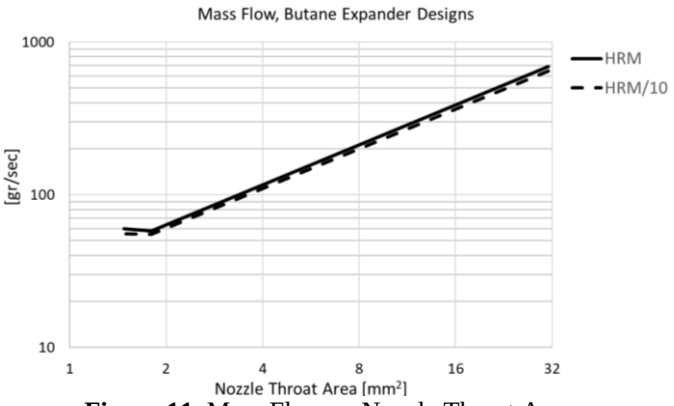

Figure 11. Mass Flow vs Nozzle Throat Area

Regarding the turbine total-to-total efficiency (Equation 6), the optimal rotational speed for maximum efficiency varies also as a function of the rate of phase change and nozzle throat area (Figure 13).

$$\eta_{total\_to\_total} = \frac{H_o(Inlet) - H_o(Outlet)}{H_o(Inlet) - H_o(Outlet_{Isentropic})} \qquad (6)$$

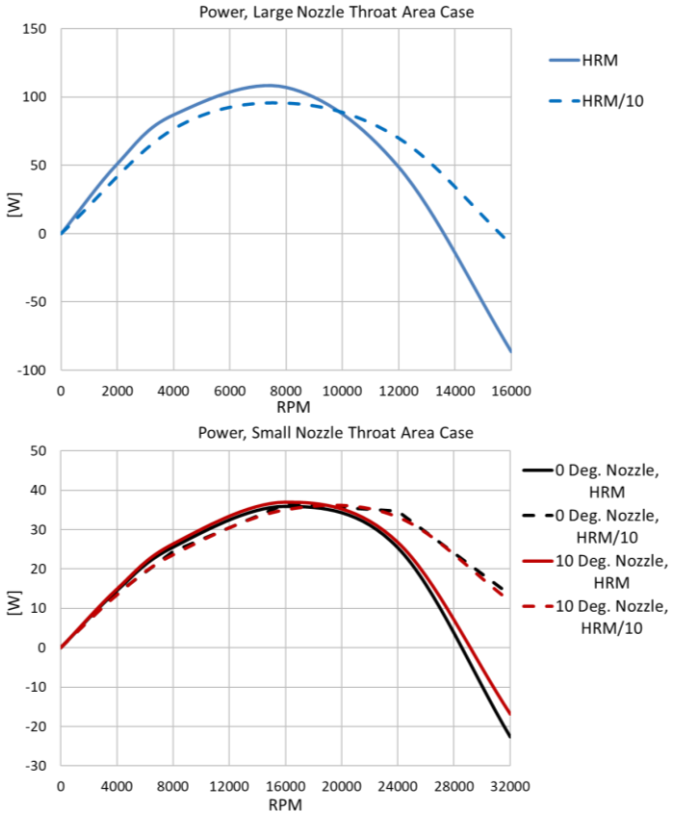

Figure 12. Power vs RPM

Nozzle angle again seems not to effect strongly the efficiency curve for the entire RPM range. The HRM/10 cases have maximum efficiency values at higher RPMs, compared to the original HRM, because the phase change location moves further upstream. It's a similar behavior as the smaller torque slope observed in Figure 10. Furthermore the small nozzle thoat area leads to an increased efficiency curve by almost five times, compared to the large nozzle throat, due to the fact that the ratio, of the output work divided by the mass flow, is significanlty higher in that case. Although the mass flow is ten times lower, the power output is only two and a half times lower. The higher volume flow of the large nozzle has more energy in it. However the fluid-disk interaction surface area is too small to extract all of that energy, before the flow exits the expander.

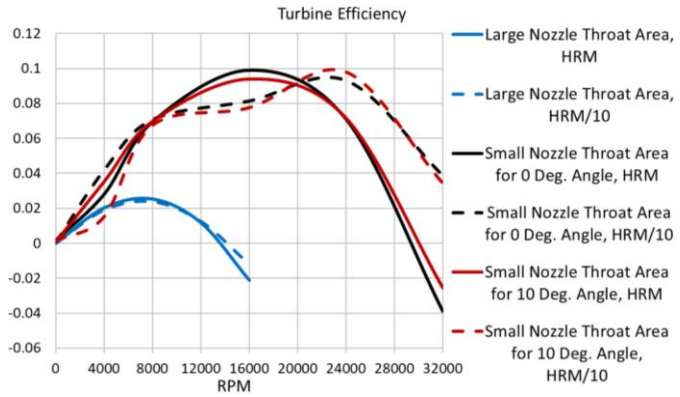

Figure 13. Efficiency vs RPM

The fact that phase change initiates further upstream, in the HRM/10 and small nozzle throat area cases, is depicted in Figure 14, where the vapour mass fraction contour in presented in the area near the nozzle.

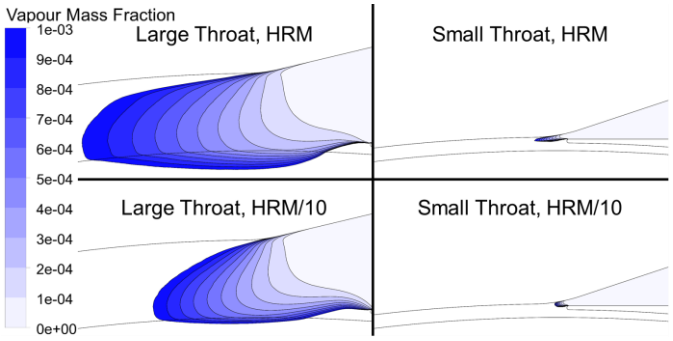

Figure 14. Vapour Mass Fraction Contour (Detailed View)

For the same maximum vapour mass fraction value of 1%, it can be observed that in the HRM/10 case the phase change is located upstream compared to the original HRM. Also important to notice is that the difference between the HRM and HRM/10 configuration has a smaller shift in the phase change than between the nozzle throat areas.

The reason for the more rapid torque drop for the case with the larger nozzle throat area, is shown in Figure 15, where the circumferential mass flow averaged circumferential relative velocity is presented. As RPM increases, the point at which the phase change starts moves downstream into the gap between the disks (Figure 18). Given the large difference in the densities of the liquid and vapour, this results in negative relative velocities at high RPM, in a region that is near the tip of the disks. This region acts as a brake on the disk.

Already at 8'000 RPM, negative relative circumferential velocities appear near the tip of the disk for the expander design with the large nozzle throat area. The same behavior also exists for the 0 and 10 Deg. cases of the smaller nozzle throat area, where negative relative velocities make their appearance around 24'000 RPM. Because of the increased nozzle throat area and resulting higher mass flow in the first case, phase change starts further downstream compared to the other cases. Comparing the 0 Deg. and 10 Deg. nozzle design, it can be observed that the relative velocities have minor differences and as a result of that, torque essentially remains the same. For the HRM/10 simulations, the model timescale factor is decreased by a factor of 10, which means that the phase change process moves upstream.

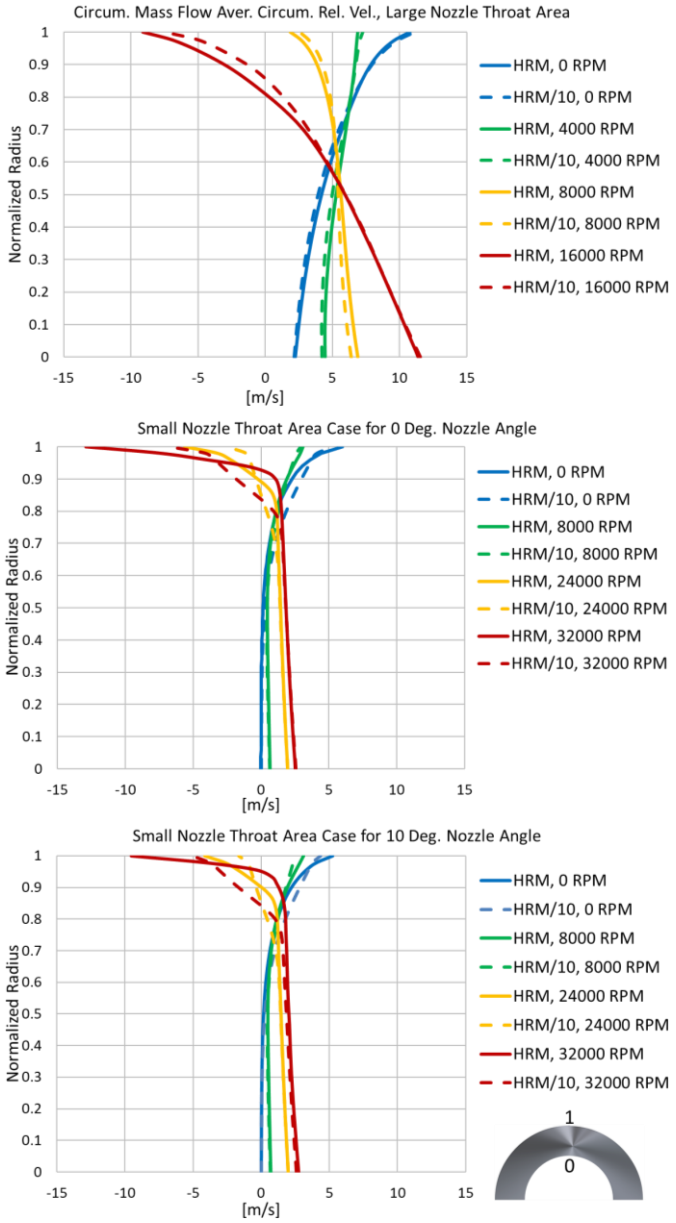

Figure 15. Rotor Relative Velocity

The effect of this is to increase slightly the negative relative circumferential velocities, postponing this braking effect to a higher RPM. The primary reason that the phase change is pushed downstream (Figure 18), when rotational speed increases, relates to the influence of the centrifugal forces, produced by the vortical flow between the disks, on the back pressure of the flow exiting the nozzle. As the rotational speed increases, the centrifugal forces increase the pressure drop across the rotor.

This is illustrated in the top chart of Figure 16. As the RPM increases, the static pressure at the inlet of the disk increases by as much as 50% for the HRM simulations. The predicted increase of pressure at the inlet of the disk versus RPM for the HRM/10 calculations is smaller, of the order of 20%, since the phase change is closer to equilibrium and hence isn't pushed as far downstream.

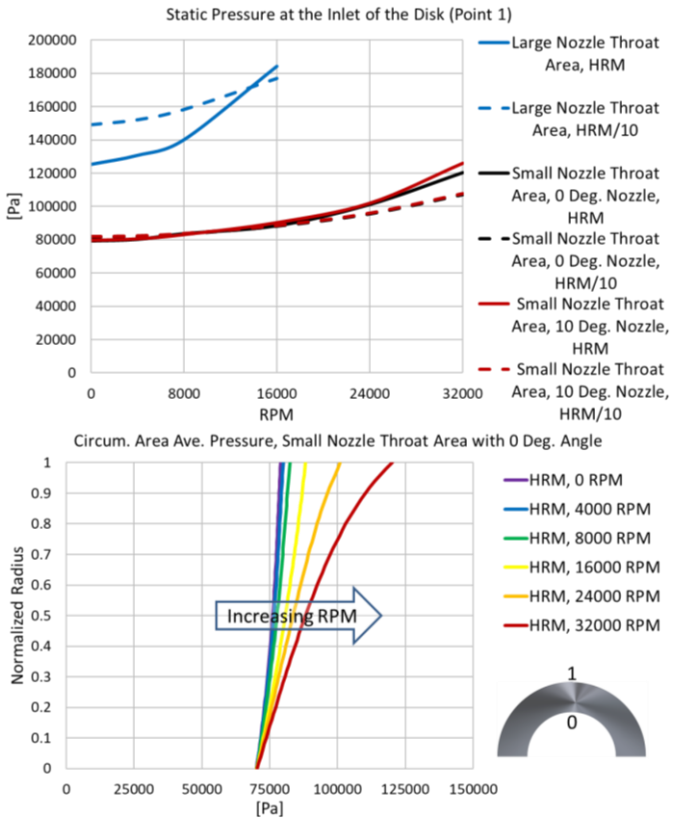

Figure 16. Pressure Distribution

In the bottom chart of the Figure 16 a typical radial profile of the pressure distribution, inside of the turbine rotor for various RPMs, is depicted. This can be visualized better in Figure 17, where pressure contours are shown for the case with the smaller nozzle throat area with 0 Deg. nozzle angle. Only a small pressure drop takes place inside the rotor at 0 RPM, but as the rotational speed increases, this effect intensifies and results in a significant pressure drop across the rotor. For this particular case at 32'000 RPM almost 12.5 % of the total expansion occurs across the rotor.

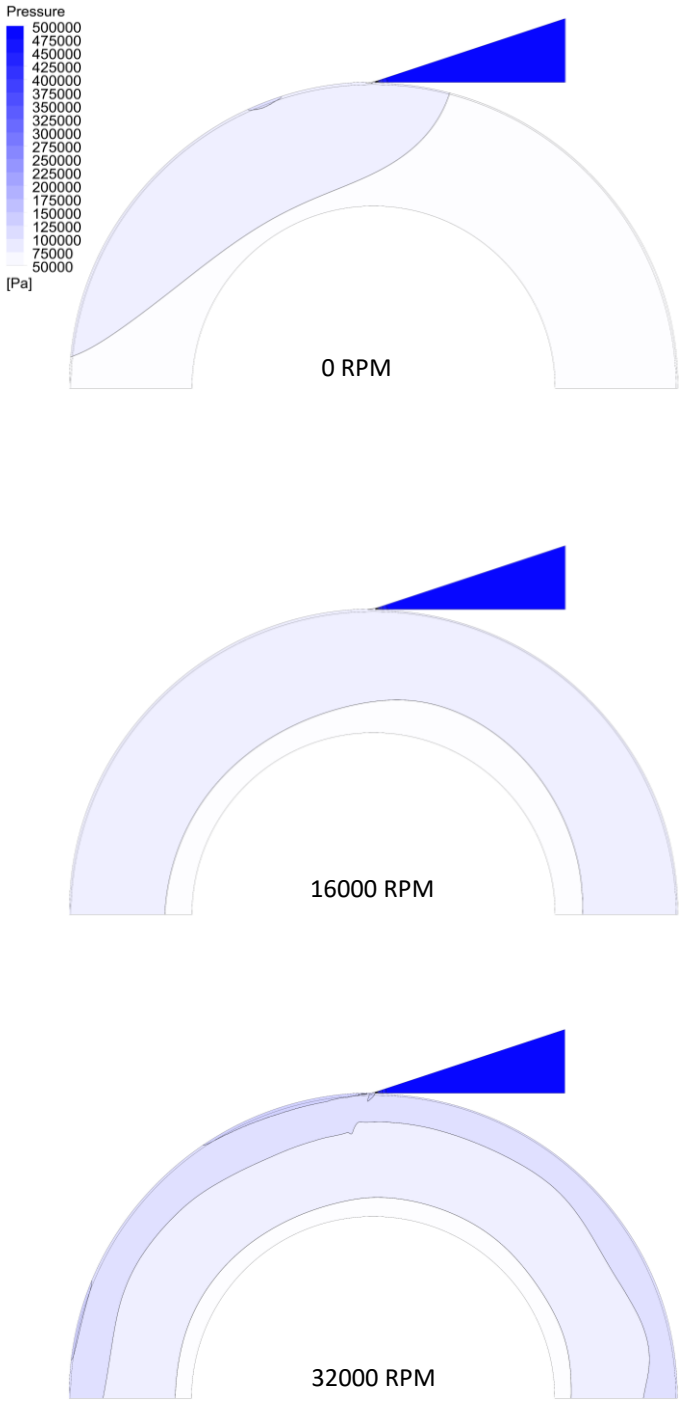

Figure 17. Static Pressure in the Expander

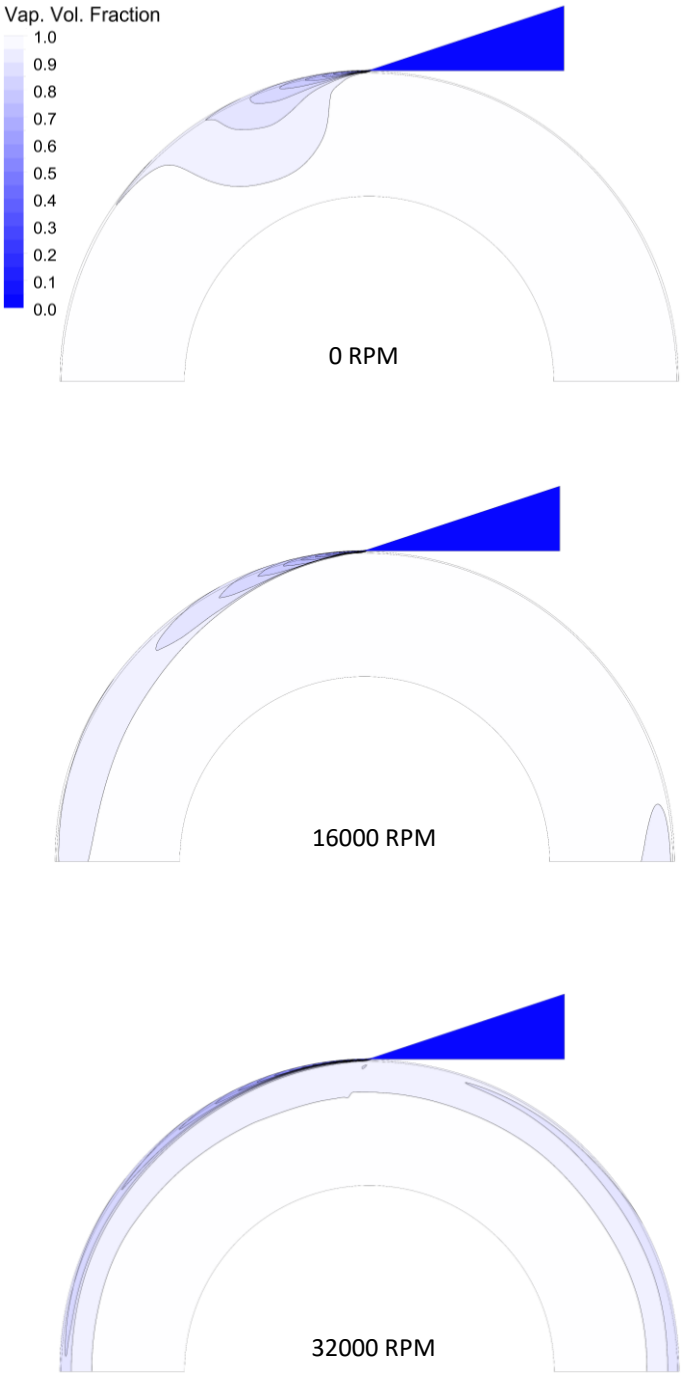

Figure 18. Vapour Volume Fraction inside the Expander

5. CONCLUSIONS

A novel application of a butane Tesla turbine for the expansion of a heat pump or refrigeration cycle is explored numerically in this study, in preparation for the development of such a concept for testing. Main goal of the study is to assess the qualitative impact of the phase change on the performance of the turbine. The analysis showed that the presence of a dense cloud of liquid droplets in the flow between the disks is expected to produce a significant pressure drop across the rotor as RPM increases, which moves the phase change further downstream and significantly reduces the performance of the turbine. Given the large difference in the densities of the liquid and vapour phase at high rotational speeds, this results in negative relative velocities in the region near the tip of the disks. This region acts as a brake on the disk, reducing torque. However a decreased nozzle throat area seems to improve the performance of the Tesla expander, since it moves the phase change upstream. The nozzle angle for the range considered, did not have a big impact on the turbine performance. It is suspected that the rapid expansion of the flow downstream of the nozzle, due to phase change, causes this flow to turn and follow the gap between the casing and the disk, which has a larger flow area. The rate of phase change has a significant impact on the turbine performance. It is critical to avoid phase change downstream of the nozzle, since significant volume fractions of liquid will enter the rotor. This will reduce the circumferential velocities and act as a brake on the disk. Future steps in that direction include optimizing the nozzle design, to ensure that most of the phase change occurs within the nozzle and/or introducing liquid extraction ports, to remove as much liquid as possible at the outer radius of the disk. By removing the liquid phase, back pressure produced by the centrifugal forces within the disk would be reduced, improving the performance of the turbine. Static testing, which will help properly validate the modelling approach utilized here, is expected to start shortly and should confirm the predictions of the rate of phase change, as well as provide insight into the diameter of droplets formed in the flow.

ACKNOWLEDGEMENTS

This project has received funding from the European Union's Horizon 2020 research and innovation programme under grant agreement No 764706, PUMP-HEAT project (https://www.pumpheat.eu/).

REFERENCES

[1] R.A. Spezia, A. Traverso, S. Barberis, L. Larosa and P. Silvestri. "World Patent WO2018/127445A1." (2018).

[2] N. Tesla. "Patent US 1061206." (1913).

[3] R. Steidel and H. Weiss. "Performance Test of a Bladeless Turbine for Geothermal Applications." (1976).

[4] E.G. Engelbrecht, Z. Giakoumis, S. Sidiropoulos, A. Chasoglou and N. Chokani. "Modelling phase change in a novel turbo expander for application to heat pumps and refrigeration cycles." *SUstainable PolyEnergy generation and HaRvesting Conference*. Vol. 113 (2019).

[5] F.R. Menter. "Two-equation eddy-viscosity turbulence models for engineering applications." *AIAA Journal* Vol. 32 No.8 (1994).

[6] S. Negro and G.M. Bianchi. “Superheated fuel injection modeling: An engineering approach.” *International Journal of Thermal Sciences.* Vol. 50 No. 8 (2011): pp. 1460-1471.

[7] M. Moulai, R. Grover, S. Parrish, and D. Schmidt. "Internal and Near-Nozzle Flow in a Multi-Hole Gasoline Injector Under Flashing and Non-Flashing Conditions." *SAE Technical Paper* No. 2015-01-0944 (2015).

[8] E.T. Baldwin, R.O. Grover, S.E. Parrish, D.J. Duke, K.E. Matusik, C.F. Powell, A.L. Kastengren and D.P. Schmidt. “String flash-boiling in gasoline direct injection simulations with transient needle motion.” *International Journal of Multiphase Flow.* Vol. 87 (2016): pp. 90-101.

[9] P. Strek, D. Duke, A. Swantek and A. Kastengren. "X-Ray Radiography and CFD Studies of the Spray G Injector." *SAE Technical Paper* No. 2016-01-0858 (2016).

[10] K. Saha, S. Som, M. Battistoni, Y. Li, S. Quan and P.K. Senecal. “Modeling of Internal and Near-Nozzle Flow for a GDI Fuel Injector.” *Proceedings of the ASME 2015 Internal Combustion Engine Division Fall Technical Conference* ICEF2015-1112 (2015).

[11] K. Saha, S. Som, M. Battistoni, Y. Li, E. Pomraning amd P.K. Senecal. “ Numerical Investigation of Two-phase Flow Evolution of In- and Near-nozzle Regions of a Gasoline Direct Injection Engine During Needle Transients.” *SAE Technical Paper* No. 2016-01-0870 (2016).

[12] K. Saha, S. Som and M. Battistoni. “Investigation of homogeneous relaxation model parameters and their implications on GDI spray formation.” *Atomization and Sprays* Vol. 27 No. 4 (2017): pp. 345-365.

[13] K. Saha, S. Quan, M. Battistoni, and P. Senecal. “Coupled Eulerian Internal Nozzle Flow and Lagrangian Spray Simulations for GDI Systems.” *SAE Technical Paper* No.2017-01-0834 (2017).

[14] S.K. Rachakonda, Y. Wang and D.P. Schmidt. “Flash-boiling initialization for spray simulations based on parametric studies” *Atomization and Sprays* Vol. 28 No. 2 (2018).

[15] Z. Bilicki and J. Kestin “Physical Aspects of the Relaxation Model in Two-Phase Flow.” *Proceedings of the Royal Society of London. Series A, Mathematical and Physical Sciences.* Vol. 428 No. 1875 (1990): pp.379-397.

[16] P. Downar-Zapolski, Z. Bilicki, L.Bolle and J. Franco. “The non-equilibrium relaxation model for one-dimensional flashing liquid flow.” *International Journal of Multiphase Flow.* Vol. 22 No.3 (1996): pp. 473-483.

[17] M. Reocreux. *“*Contribution a l’etude des debits critiques en ecoulement diphasique eauvapeur*.” PhD Thesis.* Université Scientifique et Medicale de Grenoble (1974).

[18] B.S. Park and S.Y. Lee. “Experimental Investigation of the Flash Atomization Mechanism.” *Atomization and Sprays.* Vol. 4 (1994): pp 159-179.

[19] Y. Liao and D. Lucas, “Computational modelling of flash boiling flows: A literature survey” *International Journal of Heat and Mass Transfer*. Vol. 111 (2017): pp 246-265.

[20] A. Traverso, F. Reggio, P. Silvestri, S. Rizzo. G. Engelbrecht and A. Chasoglou. “Two-phase flow expansion: development of an innovative test-rig for flow characterization and CFD validation.” *SUstainable PolyEnergy generation and HaRvesting Conference*. Vol. 113 (2019).

[21] V. N. Blinkov, O. C. Jones and B. I. Nigmatulin. “Nucleation and flashing in nozzles—2. Comparison with experiments using a five-equation model for vapor void development.” *International Journal of Heat and Mass Transfer*. Vol. 19 (1993): pp 965-986.

[22] G. A. Pinhasi, A. Ulmann, A. Dayan, “Modeling of flashing two-phase flow.” *Reviews in Chemical Engineering.* Vol. 21 (2005): pp 133-264.

[23] H. Miyamoto, K. Watanabe, “Thermodynamic Property Model for Fluid-Phase n-Butane” *International Journal of Thermophysics.* Vol. 22 No. 2 (2011): pp. 459-475